Available online at www.sciencedirect.com
SCIENCE DIRECT®
Chaos, Solitons and Fractals 20 (2004) 277–288
CHAOS SOLITONS & FRACTALS
www.elsevier.com/locate/chaos

Generating two simultaneously chaotic attractors with a switching piecewise-linear controller

Zuohuan Zheng [a], Jinhu Lü [b,*], Guanrong Chen [c], Tianshou Zhou [d], Suochun Zhang [a]

[a] *Institute of Applied Mathematics, Academy of Mathematics and System Sciences, Chinese Academy of Sciences, Beijing 100080, China*
[b] *Institute of Systems Science, Academy of Mathematics and System Sciences, Chinese Academy of Sciences, Beijing 100080, China*
[c] *Department of Electronic Engineering, City University of Hong Kong, Hong Kong*
[d] *Department of Mathematical Sciences, Tsinghua University, Beijing 100084, China*

Accepted 23 June 2003

Abstract

It has been demonstrated that a piecewise-linear system can generate chaos under suitable conditions. This paper proposes a novel method for simultaneously creating two symmetrical chaotic attractor—an upper-attractor and a lower-attractor—in a 3D linear autonomous system. Basically dynamical behaviors of this new chaotic system are further investigated. Especially, the chaos formation mechanism is explored by analyzing the structure of fixed points and the system trajectories.
© 2003 Elsevier Ltd. All rights reserved.

1. Introduction

Chaos is a very interesting non-linear phenomenon. It has been demonstrated that chaos is actually useful and can also be well controlled. Over the last decade, the intensive study of chaotic dynamics has gradually evolved from the traditional trend of understanding and analyzing chaos to the new tasks of controlling and utilizing it [1–10]. Especially, there has been increasing interest in exploiting chaotic dynamics for high-tech and real engineering applications. Recently, many efforts have been devoted to effectively generating chaos by simple control and design methods, such as switching piecewise-linear controllers [6,8,10] and chaotic circuits design [4,5,11–13].

In 2002, Lü and Chen found a new chaotic attractor by linear feedback control [9,14–18], called Lü attractor by others [19–21]. Nowadays, creating *n*-scroll chaotic attractors in (modified) Chua's circuits has become a matured technique [11,12]. Similarly, piecewise-linear functions can easily generate various chaotic attractors [6,8,10]. Motivated by many similar examples, Lü and Chen introduced a switching piecewise-linear controller [9], which can generate chaos from a 3D linear autonomous system within a wide range of parameter values. In fact, the simple analog chaos generators have strong capability of chaos generation.

In this paper, we propose a new method for simultaneously generating two symmetrical chaotic attractors via switching control based on [8]. The key is to reconstruct the controller. More precisely, we introduce a new switching scheme, a switching piecewise-linear controller, which can simultaneously create two chaotic attractors—an upper-attractor and a lower-attractor, from a 3D linear autonomous system. Moreover, basically dynamical behaviors of the new chaotic system will be investigated in some detail, by employing some mathematical tools used in [14,22–24].

* Corresponding author.
E-mail addresses: lvjinhu@mail.amss.ac.cn (J. Lü), gchen@ee.cityu.edu.hk (G. Chen).

0960-0779/$ - see front matter © 2003 Elsevier Ltd. All rights reserved.
doi:10.1016/S0960-0779(03)00376-X

Particularly, the formation mechanism of chaos will be further explored by analyzing the structure of the fixed points and the system trajectories.

2. A new chaotic system with switching controller

Consider the following 3D linear controlled system:

$$\dot{X} = AX + f(X), \tag{1}$$

where

$$A = \begin{pmatrix} a & b & 0 \\ -b & a & 0 \\ 0 & 0 & c \end{pmatrix},$$

with a switching piecewise-linear controller

$$f(X) = \begin{cases} k\begin{pmatrix} -x \\ -y \\ d \end{pmatrix}, & \text{if } z + \sqrt{x^2 + y^2} > k, \\ 0, & \text{otherwise}, \end{cases} \tag{2}$$

where a, b, c, d, k are real parameters. The system (1) and (2) can generate chaos within a wide range of parameter values [8].

To make system (1) simultaneously generate two chaotic attractors, the controller (2) is redesigned as the following switching piecewise-linear controller:

$$f(X) = \begin{cases} k\begin{pmatrix} -x \\ -y \\ d \end{pmatrix}, & \text{if } z > 0,\ z + \sqrt{x^2 + y^2} > k, \\ m\begin{pmatrix} -x \\ -y \\ e \end{pmatrix}, & \text{if } z < 0,\ z - \sqrt{x^2 + y^2} < -m, \\ 0, & \text{otherwise}, \end{cases} \tag{3}$$

where a, b, c, d, e, k, m are real parameters.

The controller (3), embedded in system (1), is switched on, when the state variables travel through the manifolds $z + \sqrt{x^2 + y^2} = k(z > 0)$ and $z - \sqrt{x^2 + y^2} = -m(z < 0)$ within the state space. These two switchings generate simultaneously two chaotic attractors—an upper-attractor and a lower-attractor, as shown in Fig. 1, when $a = 3$, $b = 20$,

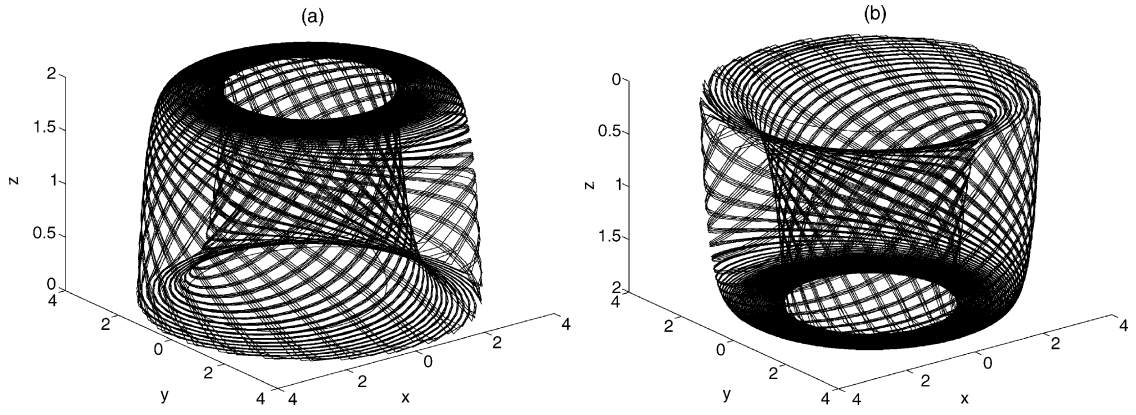

Fig. 1. The upper and lower chaotic attractors generated by the switching controller (3).

$c = -20$, $d = 10$, $e = -10$, $k = 4$, and $m = 4$. The maximum Lyapunov exponents of the two chaotic attractors are both LE = 1.4374.

A closer look at the controller (3) reveals that it has two switching manifolds: one is $z + \sqrt{x^2 + y^2} = k(z > 0)$, and the other is $z - \sqrt{x^2 + y^2} = -m(z < 0)$. These two switching manifolds are responsible for the generation of two chaotic attractors: The switching manifold $z + \sqrt{x^2 + y^2} = k(z > 0)$ is responsible for generating the upper-chaotic attractor; while the switching manifold $z - \sqrt{x^2 + y^2} = -m(z < 0)$ creates the lower-chaotic attractor.

3. Basically dynamical behaviors

Basically dynamical behaviors, such as symmetry and dissipativity, of the system (1) under the control of the switching piecewise-linear controller (3), are further investigated here from a theoretical point of view.

3.1. Symmetry and invariant set

Obviously, system (1), controlled by the switching piecewise-linear controller (3), has a natural symmetry under the coordinates transform $(x, y, z) \to (-x, -y, z)$, which persists for all values of the system parameters.

Obviously, $z = 0$ is the invariant manifold of system (1), denoted by M_1. There exists a unique fixed point, $S_0(0, 0, 0)$, on the invariant manifold M_1 for system (1). Let $V = x^2 + y^2$ on the invariant manifold M_1, then

$$\dot{V} = 2x\dot{x} + 2y\dot{y} = 2a(x^2 + y^2) = 2aV.$$

Thus, $V(t) = V(0)e^{2at}$. If $a = 0$, then S_0 is a center point; if $a \neq 0$, then S_0 is a focus point; if $a > 0$, then S_0 is unstable (and in this case, if $V(0) \geqslant 0$, then $V(t) \to +\infty$ as $t \to +\infty$ but $V(t) \to 0$ as $t \to -\infty$); if $a < 0$, then S_0 is stable (and in this case, if $V(0) \geqslant 0$, then $V(t) \to 0$ as $t \to +\infty$ and $V(t) \to +\infty$ as $t \to -\infty$), as summarized in Fig. 2. Therefore, $\mathbf{R}^3$ can be decomposed into three invariant subsets: M_1, $M_2 = \{(x, y, z) \in \mathbf{R}^3 | z > 0\}$, and $M_3 = \{(x, y, z) \in \mathbf{R}^3 | z < 0\}$.

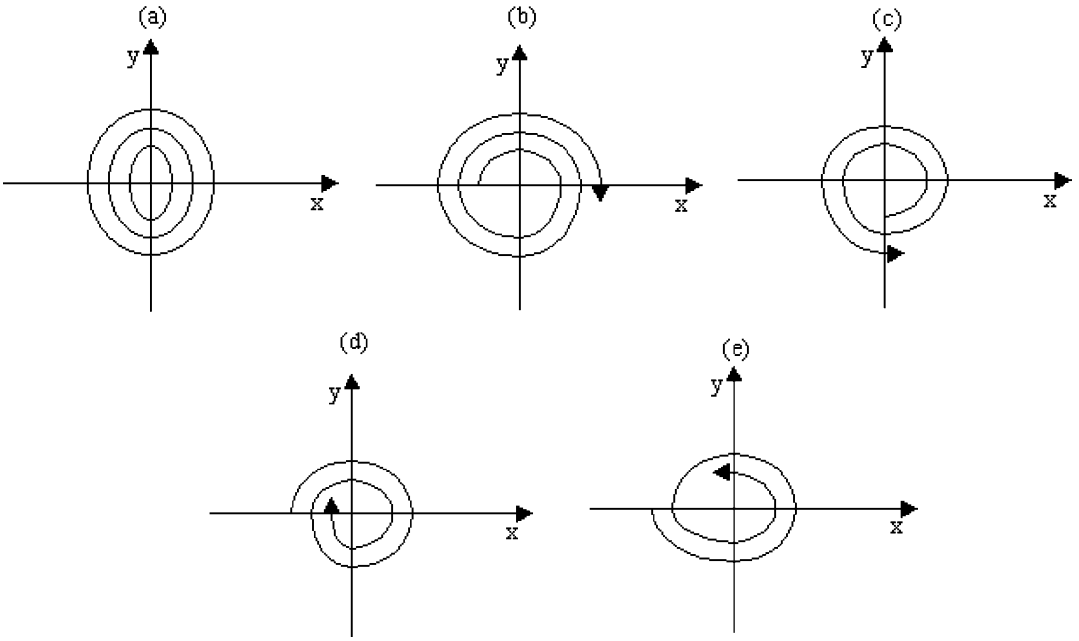

Fig. 2. The structure of trajectory in the neighborhood of the equilibrium point S_0 on M_1: (a) $a = 0$; (b) $a > 0$, $b > 0$; (c) $a > 0$, $b < 0$; (d) $a < 0$, $b > 0$; (e) $a < 0$, $b < 0$.

3.2. Dissipativity

In the following, assume that $a > 0$, $c < -2a$, $k > 0$, and $m > 0$.

The variation of the volume $V(t)$ of a small element, $\delta\Omega(t) = \delta x \delta y \delta z$ in the state space, is determined by the divergence of the flow:

$$\nabla V = \frac{\partial \dot{x}}{\partial x} + \frac{\partial \dot{y}}{\partial y} + \frac{\partial \dot{z}}{\partial z},$$

which is

$$\nabla V = \begin{cases} 2a + c - 2k < 0, & \text{for } z > 0,\ z + \sqrt{x^2 + y^2} > k, \\ 2a + c - 2m < 0, & \text{for } z < 0,\ z - \sqrt{x^2 + y^2} < -m, \\ 2a + c < 0, & \text{otherwise.} \end{cases}$$

Therefore, system (1) is dissipative at an exponential contraction rate:

$$\delta\Omega(t) = \begin{cases} e^{2a+c-2k}, & \text{for } z > 0,\ z + \sqrt{x^2 + y^2} > k, \\ e^{2a+c-2m}, & \text{for } z < 0,\ z - \sqrt{x^2 + y^2} < -m, \\ e^{2a+c}, & \text{otherwise.} \end{cases}$$

As a result, a volume element V_0 is contracted by the flow into a volume element $V_0 e^{\nabla V t}$ in time t. Namely, each volume containing the system trajectories shrinks to zero as $t \to \infty$ at an exponential rate, ∇V, which is independent of x, y, z. Thus, all system orbits will ultimately be confined to a specific subset of zero volume and the asymptotic motion settles onto an attractor.

4. Fixed point and the global attractive region

4.1. Fixed point of the controlled system

Suppose that $a = b = 0$. Then, all the points in the invariant manifold $M_1 = \{(x, y, z) \in \mathbf{R}^3 | z = 0\}$ are the fixed points of system (1).

(1) If $a = b = c = 0$ and k, d, m, e are non-zero, then the set of all the fixed points is $M_1 \cup \{(x, y, z) \in \mathbf{R}^3 | z > 0, z + \sqrt{x^2 + y^2} \leqslant k\} \cup \{(x, y, z) \in \mathbf{R}^3 | z < 0, z - \sqrt{x^2 + y^2} \geqslant -m\} = G_1$.

If $k < 0$ and $m < 0$, then $G_1 = M_1$. Fig. 3(a) shows the structure of system (1) for $d > 0$ and $e > 0$; Fig. 3(b) displays the structure of system (1) for $d > 0$ and $e > 0$; Fig. 3(c) shows the structure of system (1) for $d < 0$ and $e < 0$; Fig. 3(d) displays the structure of system (1) for $d < 0$ and $e > 0$.

(2) If $a = b = c = k = 0$ and $me \neq 0$, then the set of all the fixed points are $G_2 = \{(x, y, z) \in \mathbf{R}^3 | z \geqslant 0\} \cup \{(x, y, z) \in \mathbf{R}^3 | z < 0, z - \sqrt{x^2 + y^2} \geqslant -m\}$.

If $m < 0$, then $G_2 = \{(x, y, z) \in \mathbf{R}^3 | z \geqslant 0\}$. Fig. 4(a) shows the structure of the trajectories of system (1) for $e < 0$; Fig. 4(b) displays the structure of the trajectories of system (1) for $e > 0$. For other degenerative cases, one can draw similar structure graphs for trajectories of system (1).

(3) If $b \neq 0$, $c \neq 0$, $m > 0$, and $k > 0$, then:

(i) If $-\frac{d}{c} > 1$ and $\frac{e}{c} > 1$, then system (1) has three equilibria: $S_0(0, 0, 0)$, $S_1(0, 0, -\frac{kd}{c})$ and $S_2(0, 0, -\frac{me}{c})$;
(ii) If $-\frac{d}{c} < 1$ and $\frac{e}{c} < 1$, then system (1) has unique equilibrium point: $S_0(0, 0, 0)$;
(iii) If $-\frac{d}{c} > 1$ and $\frac{e}{c} < 1$, then system (1) has two equilibria: $S_0(0, 0, 0)$, $S_1(0, 0, -\frac{kd}{c})$;
(iv) If $-\frac{d}{c} < 1$ and $\frac{e}{c} > 1$, then system (1) has two equilibria: $S_0(0, 0, 0)$ and $S_2(0, 0, -\frac{me}{c})$.

Next, consider the equilibrium $S_0(0, 0, 0)$. The system Jacobian J at this point is

$$J = \begin{pmatrix} a & b & 0 \\ -b & a & 0 \\ 0 & 0 & c \end{pmatrix}, \tag{4}$$

which has the eigenvalues $\lambda_{1,2} = a \pm bi$ and $\lambda_3 = c$. Therefore, the stability of the equilibrium $S_0(0, 0, 0)$ can be classified as follows:

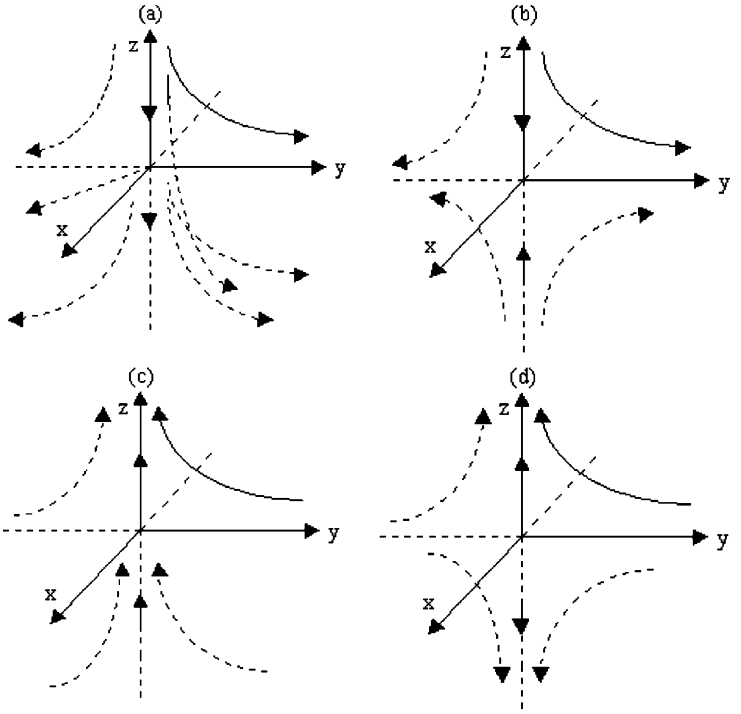

Fig. 3. The structure of the trajectories of system (1): (a) $d > 0$, $e > 0$; (b) $d > 0$, $e < 0$; (c) $d < 0$, $e < 0$; (d) $d < 0$, $e > 0$.

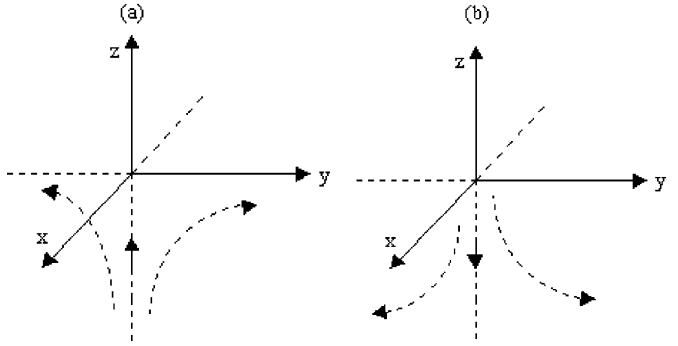

Fig. 4. The structure of trajectory for system (1): (a) $e < 0$; (b) $e > 0$.

(i) If $a > 0$ or $c > 0$, then this equilibrium is unstable. Fig. 5(a)–(b) show the structure of the trajectories in the neighborhood of $S_0(0,0,0)$ for $a > 0$ and $c > 0$; Fig. 5(c)–(d) display the structure of the trajectories in the neighborhood of $S_0(0,0,0)$ for $a > 0$ and $c < 0$; Fig. 5(e)–(f) show the structure of the trajectory in the neighborhood of $S_0(0,0,0)$ for $a < 0$ and $c > 0$.

(ii) If $a < 0$ and $c < 0$, then this equilibrium is stable. Fig. 5(g)–(h) display the structure of the trajectory in the neighborhood of $S_0(0,0,0)$.

Moreover, note that for $c < 0$, $a = 0$ is a Hopf bifurcation point.

Similarly, when $-\frac{d}{c} > 1$, for the equilibrium $S_1(0,0,-\frac{kd}{c})$, the system Jacobian is

$$J = \begin{pmatrix} a-k & b & 0 \\ -b & a-k & 0 \\ 0 & 0 & c \end{pmatrix}, \tag{5}$$

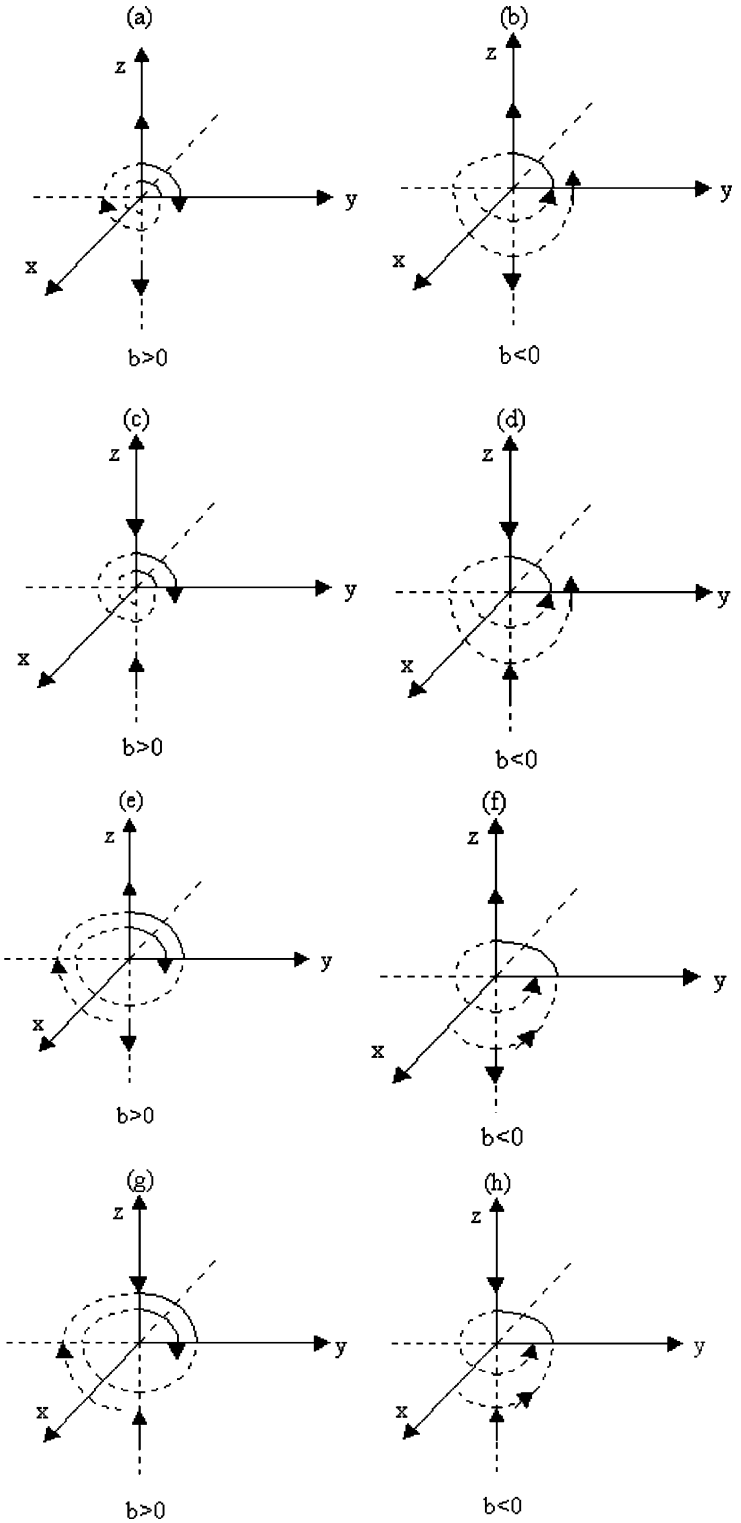

Fig. 5. The structure of the system trajectories in the neighborhood of S_0: (a)–(b) $a > 0$, $c > 0$; (c)–(d) $a > 0$, $c < 0$; (e)–(f) $a < 0$, $c > 0$; (g)–(h) $a < 0$, $c < 0$.

and its eigenvalues are $\lambda_{1,2} = a - k \pm bi$ and $\lambda_3 = c$. Obviously, for $c < 0$, $a = k$ is a Hopf bifurcation point. The stability of this equilibrium, $S_1(0, 0, -\frac{kd}{c})$, is classified as follows:

(i) If $a > k$ and $c > 0$, then S_1 is unstable. Fig. 6(a)–(b) show the structure of the trajectories in the neighborhood of S_1.
(ii) If $a > k$ and $c < 0$, then S_1 is unstable. Fig. 6(c)–(d) display the structure of the trajectories in the neighborhood of S_1.
(iii) If $a < k$ and $c > 0$, then S_1 is unstable. Fig. 6(e)–(f) show the structure of the trajectory in the neighborhood of S_1.
(iv) If $a < k$ and $c < 0$, then S_1 is stable. Fig. 6(g)–(h) display the structure of the trajectory in the neighborhood of S_1.

Similarly, when $\frac{e}{c} > 1$, for the equilibrium $S_2(0, 0, -\frac{me}{c})$, the system Jacobian is

$$J = \begin{pmatrix} a-m & b & 0 \\ -b & a-m & 0 \\ 0 & 0 & c \end{pmatrix} \tag{6}$$

and its eigenvalues are $\lambda_{1,2} = a - m \pm bi$ and $\lambda_3 = c$. Clearly, for $c < 0$, $a = m$ is a Hopf bifurcation point. The stability of this equilibrium, $S_2(0, 0, -\frac{me}{c})$, is classified as follows:

(i) If $a > m$ and $c > 0$, then S_2 is unstable. The structures of the trajectories in the neighborhood of S_2 are similar to Fig. 6(a)–(b).
(ii) If $a > m$ and $c < 0$, then S_2 is unstable. The structures of the trajectory in the neighborhood of S_2 are similar to Fig. 6(c)–(d).
(iii) If $a < m$ and $c > 0$, then S_2 is unstable. The structures of the trajectory in the neighborhood of S_2 are similar to Fig. 6(e)–(f).
(iv) If $a < m$ and $c < 0$, then S_2 is stable. The structures of the trajectories in the neighborhood of S_2 are similar to Fig. 6(g)–(h).

4.2. The global attractive region

For any point $A(x_0, y_0, z_0) \in \mathbf{R}^3$, let $g(t, A)$ be the solution of system for $g(0, A) = A$. Denote $g(R_0, A) = \{g(t, A) | t \in R_0\}$ for $R_0 \subset R$.

Definition 1. Suppose that $B \subset \mathbf{R}^3$. If $\forall A \in \mathbf{R}^3$, $\exists T > 0$, such that $g([T, +\infty), A) \subset B$, then B is called as the *global attractive region*.

In the following, assume that $a < 0$, $b > 0$, $c < 0$, $d > 0$, $e < 0$, $m > 0$, $k > 0$. Denote $B_1 = \{(x, y, z) | z \geqslant 0, z + \sqrt{x^2 + y^2} \leqslant k\}$, $B_2 = \{(x, y, z) | z \leqslant 0, z - \sqrt{x^2 + y^2} \geqslant -m\}$, $l_1 = -\frac{k}{c}\sqrt{c^2 + d^2}$, $l_2 = -\frac{m}{c}\sqrt{c^2 + e^2}$. Let $l_3 > l_1$, $l_4 > l_2$, such that $B_1 \subset B_3 \triangleq \{(x, y, z) | z \geqslant 0, \sqrt{x^2 + y^2 + (z + \frac{kd}{c})^2} \leqslant l_3\}$, $B_2 \subset B_4 \triangleq \{(x, y, z) | z \leqslant 0, \sqrt{x^2 + y^2 + (z + \frac{me}{c})^2} \leqslant l_4\}$. Denote $\bar{B} = B_3 \cup B_4$.

Theorem 1. *When $c < \min\{a - k, a - m\}$, then $\bar{B}$ is a global attractive region.*

Proof. $\forall A(x_0, y_0, z_0) \in \mathbf{R}^3$, when $z_0 = 0$, we have $g(R, A) \subset M_1$ and there is unique fixed point $S_0 \in M_1$ from the discussion in Section 3.

Since $a < 0$, then S_0 is a stable focus point, and the positive trajectories of all trajectories in M_1 tend to S_0. Therefore, $\exists T > 0$, such that $g([T, +\infty), A) \subset \bar{B}$.

When $z_0 > 0$, let $V = x^2 + y^2 + (z + \frac{kd}{c})^2$. For $z > 0$ and $z + \sqrt{x^2 + y^2} > k$, we have

$$\begin{aligned} \dot{V} &= 2\left[x\dot{x} + y\dot{y} + \left(z + \frac{kd}{c}\dot{z}\right)\right] = 2\left[(a-k)(x^2 + y^2) + c\left(z + \frac{kd}{c}\right)^2\right] \\ &= 2\left[(a-k)V_2 + (c + k - a)\left(z + \frac{kd}{c}\right)^2\right] \leqslant 2(a-k)V_2 \leqslant 0 \end{aligned}$$

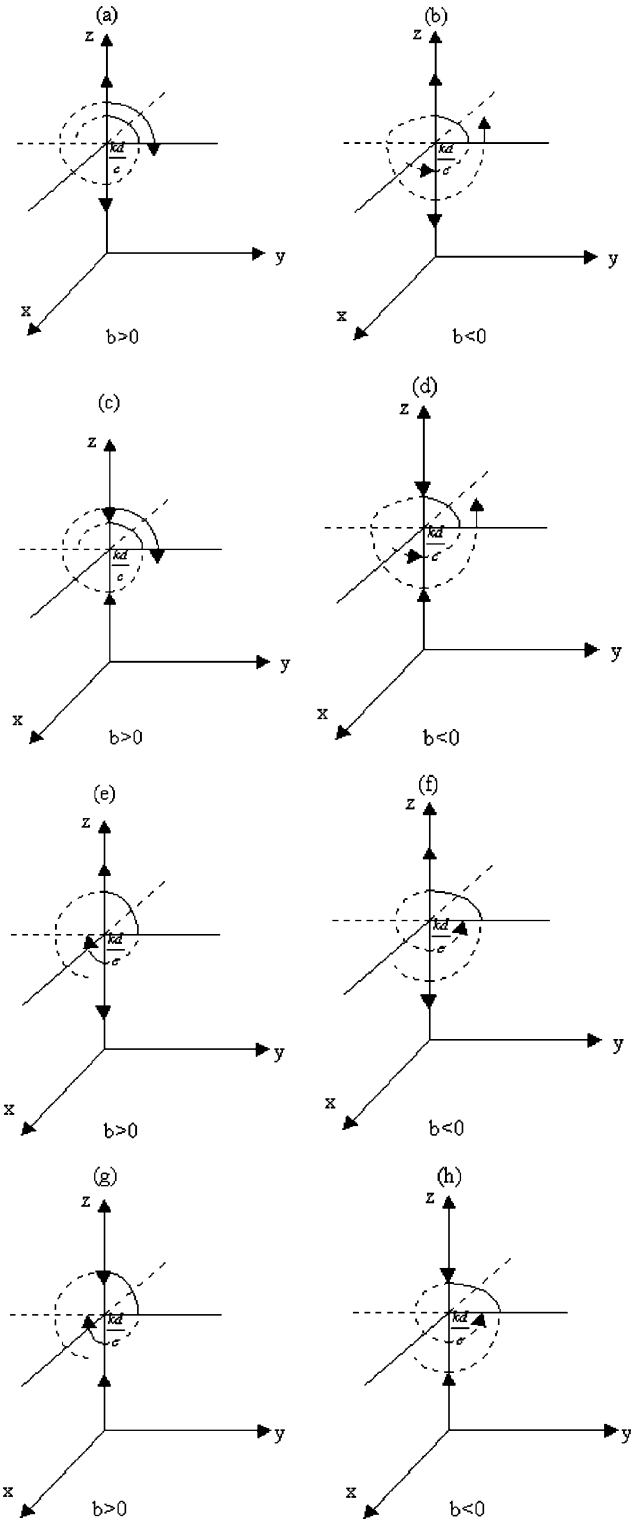

Fig. 6. The structure of the trajectories in the neighborhood of S_1: (a)–(b) $a > k$, $c > 0$; (c)–(d) $a > k$, $c < 0$; (e)–(f) $a < k$, $c > 0$; (g)–(h) $a < k$, $c < 0$.

Moreover, when $z > 0$ and $\sqrt{x^2+y^2+(z+\frac{kd}{c})^2} > l_1$, $V > 0$. Hence, $\dot{V} < 0$. Denote $A_5(x,y,z)$ be the boundary point of region $B_5 = \{(x,y,z)|z \geqslant 0, \sqrt{x^2+y^2+(z+\frac{kd}{c})^2} \leqslant l\}(l > l_1)$. When $z > 0$, A_5 is the strictly entering point according to the theorem in Ref. [23]. Therefore, when $z_0 > 0$, $\exists T > 0$, such that $g([T,+\infty),A) \subset \bar{B}$.

Similarly, when $z_0 < 0$, $\exists T > 0$, such that $g([T,+\infty),A) \subset \bar{B}$. Hence, $\bar{B}$ is a global attractive region. And the proof is completed here. □

Remarks. For the case of $a > 0$, we can get similar theorem. That is, there are local attractive regions in certain parameter region for M_2 and M_3, respectively.

5. Chaos formation mechanism

In this section, we explore the chaos formation mechanism by using the structure of trajectories and numerical simulations.

5.1. Structure of trajectory

In this subsection, assume that $a > 0$, $c < 0$, $0 < d < -c$, $c < e < 0$, $a < k \leqslant a - c$, and $a < m \leqslant a - c$. Denote four regions as: $\Sigma_1 : \{(x,y,z)|z > 0, \quad z + \sqrt{x^2+y^2} \leqslant k\}$, $\Sigma_2 : \{(x,y,z)|z > 0, \quad z + \sqrt{x^2+y^2} > k\}$, $\Sigma_3 : \{(x,y,z)|z < 0, z - \sqrt{x^2+y^2} \geqslant -m\}$, $\Sigma_4 : \{(x,y,z)|z < 0, z - \sqrt{x^2+y^2} < -m\}$.

When $z < 0$ and $z - \sqrt{x^2+y^2} \geqslant -m$, system (1) becomes

$$\begin{cases} \dot{x} = ax + by, \\ \dot{y} = -bx + ay, \\ \dot{z} = cz. \end{cases} \tag{7}$$

From the third equation of system (7), $z(t) = z(0)e^{ct}$. Thus, for $c < 0$, when $t \to +\infty$, one has $z(t) \to 0$. Let $V_1 = x^2 + y^2$, then we have

$$\dot{V}_1 = 2x\dot{x} + 2y\dot{y} = 2a(x^2+y^2) = 2aV_1.$$

Hence, $V_1(t) = V_1(0)e^{2at}$. That is, when $V_1(0) \geqslant 0$ and $t \to +\infty$, $V_1(t) \to +\infty$, so that $f(t) = z - \sqrt{x^2+y^2} \to -\infty$. So $\exists t_1 > 0$, such that $f(t_1) < -m$. Therefore, the trajectories of system (1) will go through the plane $z - \sqrt{x^2+y^2} = -m$ from the region Σ_3 and then switches into region Σ_4. After this instant, the system becomes

$$\begin{cases} \dot{x} = (a-m)x + by, \\ \dot{y} = -bx + (a-m)y, \\ \dot{z} = cz + me. \end{cases} \tag{8}$$

Let $V_2 = x^2 + y^2 + (z + \frac{me}{c})^2$, then we get

$$\begin{aligned} \dot{V}_2 &= 2[x\dot{x} + y\dot{y} + \left(z + \frac{me}{c}\right)\dot{z}] = 2\left[(a-m)(x^2+y^2) + c\left(z + \frac{me}{c}\right)^2\right] \\ &= 2\left[(a-m)V_2 + (c+m-a)\left(z + \frac{me}{c}\right)^2\right] \leqslant 2(a-m)V_2. \end{aligned}$$

Hence, $V_2(t) \leqslant V_2(0)e^{2(a-m)t} \to 0$, as $t \to +\infty$. Then, when $t \to +\infty$, $f(t) = z - \sqrt{x^2+y^2} \to -\frac{me}{c} > -m$. That is, $\exists t_2 > t_1$, such that $f(t_2) > -m$. Thus, the trajectories of system (1) will go through the plane $z - \sqrt{x^2+y^2} = -m$ from the region Σ_4 and then switches into region Σ_3.

Therefore, for any initial value (x_0, y_0, z_0), if $z_0 < 0$, then as $t \to +\infty$, the trajectories of system (1) will go through the plane $z - \sqrt{x^2+y^2} = -m$ repeatedly for infinitely many times. System (1) has different dynamical behaviors in the above different regions, Σ_3 and Σ_4. When $t \to +\infty$, system (1) changes dynamical behaviors as the trajectory goes through the two regions alternately and repeatedly. That is, the dynamical behaviors of system (1) is changing repeatedly, leading to complex dynamics such as the appearance of bifurcations and chaos.

Note that, if $z_0 < 0$, then all trajectories of system (1) remain in the above two regions: Σ_3 and Σ_4. According to the above theoretical analysis, for any initial value (x_0, y_0, z_0), if $z_0 < 0$, then system (1) has folding and stretching dynamics repeatedly, producing a chaotic attractor below the plane $z = 0$, called the lower-attractor.

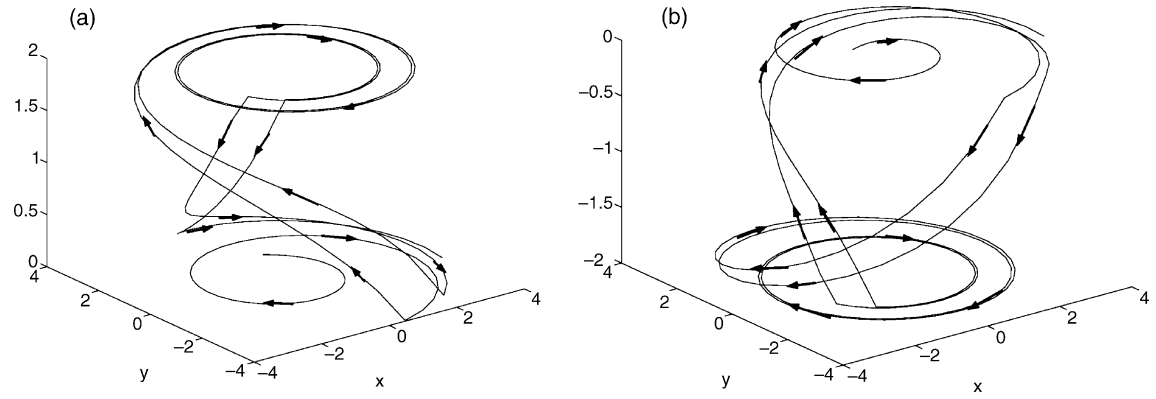

Fig. 7. The structure of trajectories for the upper and lower chaotic attractors.

Similarly, for any initial value (x_0, y_0, z_0), if $z_0 > 0$, then as $t \to +\infty$, the trajectories of system (1) go through the plane $z + \sqrt{x^2 + y^2} = k$ repeatedly for infinitely many times. Note that, if $z_0 > 0$, then all trajectories of system (1) remain in the two regions: Σ_1 and Σ_2. Furthermore, for any initial value (x_0, y_0, z_0), if $z_0 > 0$, then as $t \to +\infty$, system (1) changes dynamical behaviors when the trajectories go through the two regions: Σ_1 and Σ_2, repeatedly, producing a chaotic attractor above the plane $z = 0$, called the upper-attractor.

In summary, for any two different initial values (x_1, y_1, z_1) and (x_2, y_2, z_2), if $z_1 > 0$ and $z_2 < 0$, then system (1) may produce two different chaotic attractors—the upper-attractor and the lower-attractor—for some suitable system parameters a, b, c, d, e, k, m.

As discussed in Section 3, under condition $0 < d < -c$ and $c < e < 0$, system (1) has unique and stable equilibrium, $(0, 0, 0)$.

Suppose that $a = 3$, $b = 20$, $c = -20$, $d = 10$, $e = -10$, and $k = m = 4$. For initial value $(x_0, y_0, z_0) = (0.1, 1, 0.1)$, since $z_0 > 0$, all trajectories of system (1) remain in the invariant manifold M_2 and form a upper-chaotic attractor as shown in Fig. 1(a). Fig. 7(a) shows the directions of the trajectories for the attractor, indicated by the arrows therein. From Fig. 7(a), one can see that the trajectories run to inside of region Σ_1, and then to inside of region Σ_2, and finally back to inside of region Σ_1, and so on.

For initial value $(x_0, y_0, z_0) = (0.1, 1, -0.1)$, since $z_0 < 0$, all trajectories of system (1) remain in the invariant manifold M_3 and form a lower-attractor, as shown in Fig. 1(b). Fig. 7(b) displays the directions of the trajectories for the attractor, indicated by the arrows therein. From Fig. 7(b), one can see that the trajectories run to inside of region Σ_3, and then to inside of region Σ_4, and finally back to inside of region Σ_3, and so on.

5.2. Numerical simulations

In this section, the dynamical behaviors of the switching controlled system (1) are investigated by numerical simulations.

For the switching piecewise-linear controller (3), one can see that when $d = -e$ and $k = m$, the upper-attractor and the lower-attractor are symmetrical about the plane $z = 0$ (see Fig. 1).

Fix parameters $b = 20$, $c = -15$, $d = -e = 10$, $k = m = 6$, and let a vary. Numerical simulations show that the trajectories of system (1) converge to a sink for both $a < 0$ and $a > 6$; system has two symmetrical limit cycles for both $a = 0$ and $a = 6$ (see Fig. 8(a)–(b)); system is chaotic or chaos-like for $0.1 < a < 6$.

Fix parameters $a = 3$, $c = -15$, $d = -e = 10$, $k = m = 6$, and let b vary. Numerical simulations show that system (1) is chaotic or chaos-like for almost all values of b (see Fig. 8(c)–(d)).

Fix parameters $a = 3$, $b = 20$, $k = 8$, $d = -e = 10$, $k = m = 6$, and let c vary. The system (1) does not converge to any point for $c \geqslant 0$; it converges to a sink for $-10 < c < 0$; it is chaotic or chaos-like for $c < -10$.

6. Conclusions

This paper has introduced a new switching controller for chaos generation, which can simultaneously generate two symmetrical chaotic attractors. Basically dynamical behaviors of the switching piecewise-linear controlled system have

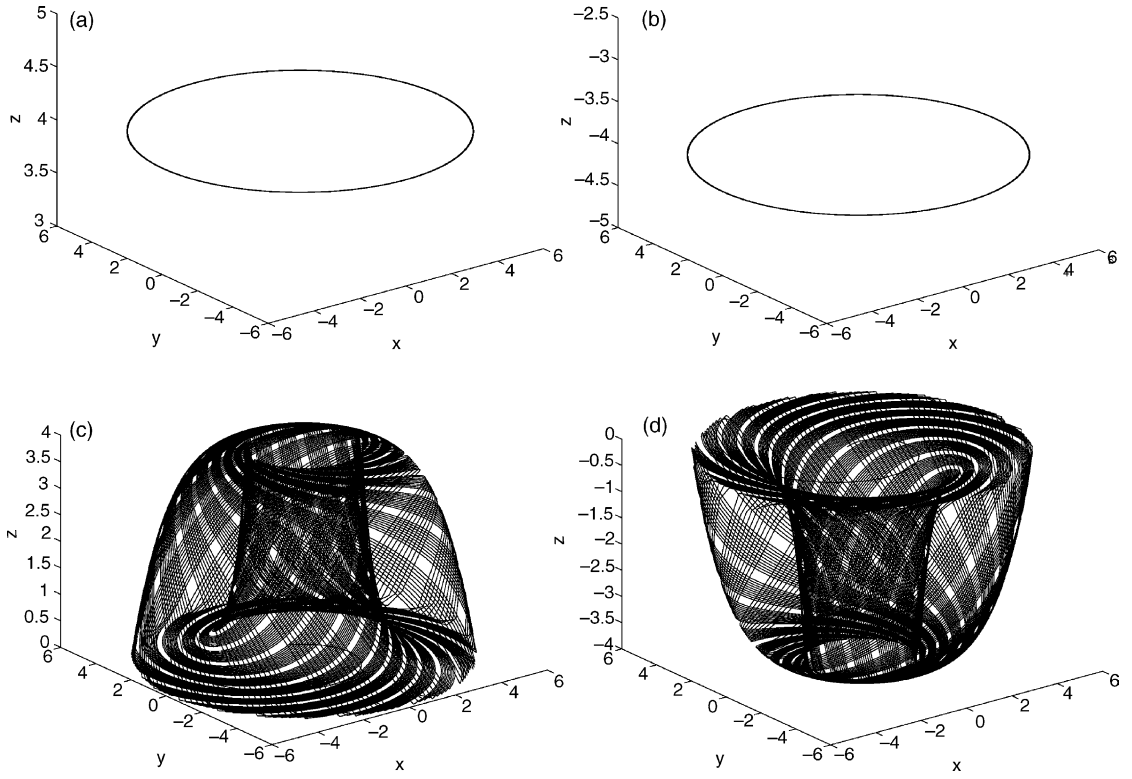

Fig. 8. Symmetrical phase portraits of system (1): (a) $a = 6$, $z_0 > 0$; (b) $a = 6$, $z_0 < 0$; (c) $b = 10$, $z_0 > 0$; (d) $b = 10$, $z_0 < 0$.

been analyzed, both theoretically and numerically. Moreover, the chaos formation mechanism of the new chaotic system has been explored by analyzing the structure of fixed points and the system trajectories.

It has been demonstrated that abundant complex dynamical behaviors can be generated by piecewise-linear functions if designed appropriately. Although this paper provides one more class of systems that fall into this category, the new finding is quite interesting both theoretically and practically, especially in the regard of possible future engineering applications of chaos generation.

Acknowledgements

This work was supported by the Hong Kong Research Grants Council under the CERG grant CityU 1004/02E, K.C. Wong Education Foundation, Hong Kong and the Chinese Postdoctoral Scientific Foundation. The authors would like to thank Professor M.S. El Naschie for some helpful suggestions.

References

[1] Chen G, Dong X. From chaos to order: methodologies, perspectives and applications. Singapore: World Scientific; 1998.
[2] Wang X, Chen G. Chaotification via arbitrarily small feedback controls: theory, method, and applications. Int J Bifur Chaos 2000;10:549–70.
[3] Wang X, Chen G, Yu X. Anticontrol of chaos in continuous-time systems via time-delayed feedback. Chaos, Solitons & Fractals 2000;10:771–9.
[4] Tang KS, Man KF, Zhong GQ, Chen G. Generating chaos via $x|x|$. IEEE Trans Circuits Syst I 2001;48:636–41.
[5] Zhong GQ, Tang KS, Chen G, Man KF. Bifurcation analysis and circuit implementation of a simple chaos generator. Latin Amer Appl Res 2001;31:227–32.
[6] Lü J. Switching control: from simple rules to complex chaotic systems. J Syst Sci Complex 2003;16(3):404–13.
[7] Lü J, Lu J, Chen S. Chaotic time series analysis and its applications. China: Wuhan University Press; 2002.

[8] Lü J, Zhou T, Chen G, Yang X. Generating chaos with a switching piecewise-linear controller. Chaos, Solitons & Fractals 2002;12:344–9.
[9] Lü J, Chen G. A new chaotic attractor coined. Int J Bifur Chaos 2002;12:659–61.
[10] Yang X, Li Q. Chaotic attractor in a simple hybrid system. Int J Bifur Chaos 2002;12:2255–6.
[11] Suykens JAK, Vandewalle J. Generation of n-double scrolls ($n = 1, 2, 3, 4, \ldots$). IEEE Trans Circuits Syst I 1993;40:861–7.
[12] Scanlan SO. Synthesis of piecewise-linear chaotic oscillators with prescribed eigenvalues. IEEE Trans Circuits Syst I 2001;48:1057–64.
[13] Yalçin ME, Suykens JAK, Vandewalle J, Özoğuz S. Families of scroll grid attractors. Int J Bifur Chaos 2002;12:23–41.
[14] Lü J, Chen G, Zhang S. Dynamical analysis of a new chaotic attractor. Int J Bifur Chaos 2002;12:1001–15.
[15] Lü J, Zhou T, Zhang S. Chaos synchronization between linearly coupled chaotic system. Chaos, Solitons & Fractals 2002;14(4):529–41.
[16] Lü J, Chen G, Zhang S. The compound structure of a new chaotic attractor. Chaos, Solitons & Fractals 2002;14(5):669–72.
[17] Chen S, Lü J. Synchronization of an uncertain unified chaotic system via adaptive control. Chaos, Solitons & Fractals 2002;14(4):643–7.
[18] Lü J, Lu J. Controlling uncertain Lü system using linear feedback. Chaos, Soliton & Fractals 2003;17(1):127–33.
[19] Yu Y, Zhang S. Controlling uncertain Lü system using backstepping design. Chaos, Soliton & Fractals 2003;15:897–902.
[20] Chen G, Lü J. Dynamical analysis, control and synchronization of the Lorenz systems family. Beijing: Science Press; 2003.
[21] Wu X, Lu J. Parameter identification and backstepping control of uncertain Lü system. Chaos, Solitons & Fractals 2003;18(4):721–9.
[22] Zheng ZH. On the limit cycles for a class of planar system. Nonlinear Anal 1995;24:605–14.
[23] Wang HF, Yu SX. Qualitative theory of ordinary differential equations. China: Guang Dong Higher Education Press; 1996.
[24] Zheng ZH. Some properties for the attractors. Sci China A 2001;44:823–8.